

A Lattice Test of $1/N_c$ Baryon Mass Relations

Elizabeth E. Jenkins,¹ Aneesh V. Manohar,¹ J.W. Negele,² and André Walker-Loud³

¹*Department of Physics, University of California at San Diego, La Jolla, CA 92093*

²*Center for Theoretical Physics, Massachusetts Institute of Technology, Cambridge, MA 02139*

³*Department of Physics, College of William and Mary, Williamsburg, VA 23187-8795*

(Dated: April 19, 2022 0:59)

$1/N_c$ baryon mass relations are compared with lattice simulations of baryon masses using different values of the light quark masses, and hence different values of $SU(3)$ flavor symmetry breaking. The lattice data clearly display both the $1/N_c$ and $SU(3)$ flavor symmetry breaking hierarchies. The validity of $1/N_c$ baryon mass relations derived without assuming approximate $SU(3)$ flavor symmetry also can be tested by lattice data at very large values of the strange quark mass. The $1/N_c$ expansion constrains the form of discretization effects; these can be suppressed by powers of $1/N_c$ by taking suitable combinations of masses.

I. INTRODUCTION

The $1/N_c$ expansion of QCD [1] is a valuable tool for studying the non-perturbative dynamics of the strong interactions [2, 3]. In the limit $N_c \rightarrow \infty$, the baryon sector of QCD has an exact *contracted* $SU(2N_F)$ spin-flavor symmetry [4]. For finite N_c , the contracted spin-flavor symmetry is broken by effects suppressed by powers of $1/N_c$ [4, 5]. The spin-flavor structure of the $1/N_c$ breaking terms is predicted at each order in the $1/N_c$ expansion [4–6]. The spin-flavor structure of many baryon properties have been derived in a systematic expansion in $1/N_c$ [7–12], and the results are in excellent agreement with experiment (for reviews, see [13, 14]).

One important application of the baryon $1/N_c$ expansion is to baryon masses [6, 15, 16]. By choosing appropriate linear combinations of the baryon masses, one can study coefficients of the baryon mass $1/N_c$ operator expansion with definite spin-flavor transformation properties. In the case of perturbative $SU(3)$ flavor symmetry breaking, the $1/N_c$ analysis gives a hierarchy of baryon mass relations in powers of $1/N_c$ and the dimensionless $SU(3)$ breaking parameter $\epsilon \propto m_s/\Lambda_\chi$ [15]. The analysis in Ref. [15] showed that the experimentally measured masses of the ground state octet and decuplet baryons exhibit the predicted hierarchy of the combined expansion in $1/N_c$ and $SU(3)$ flavor symmetry breaking. The $1/N_c$ expansion also has been used to obtain very accurate predictions for the charm and bottom baryon masses [16] (to better than 10 MeV accuracy) which have been confirmed by recent experiments. In addition, Ref. [6] derived baryon mass relations which only depend on the $1/N_c$ expansion and which are valid even if flavor $SU(3)$ is not a good approximate symmetry, i.e. for large values of the strange quark mass.

The predictions of the $1/N_c$ expansion for baryon masses are in excellent agreement with the experimental values. However, in comparing with the experimental data, one is restricted to only one value of N_c and to the physical quark mass values. Testing the predictions as a function of light quark masses and N_c is now possible with very accurate simulations of baryons using lattice

QCD.

Tremendous progress in lattice QCD has been achieved recently in the simulation of baryon masses using different values of the light quark masses. Extrapolation of baryon masses on the lattice to the physical point has reproduced the experimental values at the 1–3% level [17]. The lattice data, however, contain important additional information about the dependence of the baryon masses on the quark masses, which can be utilized. Simulations of baryon masses have been performed as a function of $SU(3)$ flavor symmetry breaking ranging from small perturbative flavor symmetry breaking to large non-perturbative flavor symmetry breaking. There are also lattice simulations at different values of N_c (though not for baryons) which are able to test N_c scaling rules [19, 20].

In this paper, we show that existing lattice simulations (at $N_c = 3$) of the ground state baryon masses already are sufficiently accurate to exhibit and test interesting features of the $1/N_c$ and $SU(3)$ flavor symmetry breaking expansions. Still more accurate simulations are needed to test the most suppressed mass combinations of the $1/N_c$ expansion, but continued improvements in lattice simulations of baryon masses are expected in the short and long term, so it should eventually be possible to test these relations as well. We discuss in this paper how present and future lattice data can be utilized to study the spin and flavor structure of baryon masses. Although we do not focus on this point here, it should eventually be possible to test the N_c scaling rules in the baryon sector by lattice simulations which vary the number of colors N_c .

An important observation is that the $1/N_c$ counting rules hold at finite lattice spacing, and so are respected by the lattice results *including* the finite lattice spacing corrections dependent on the lattice spacing a . Thus the discretization corrections are constrained by the $1/N_c$ expansion.

Lattice computations of hadron masses are done at varying values of the light quark masses m_u , m_d and m_s , usually in the isospin limit $m_u = m_d \equiv m_{ud}$. The lattice results are then extrapolated to the physical val-

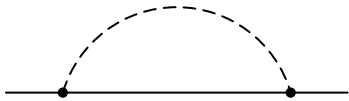


FIG. 1: One loop correction to the baryon mass due to π, K radiative corrections.

ues of m_{ud} . It has not been possible to compute hadron masses for physical values of m_{ud} yet due to the large computational time needed, since $\tau_{\text{comp}} \propto 1/m_{ud}^3$.¹ However, recently, with both algorithmic developments [21] and large parallel computing machines, there are two groups simulating at or near the physical light quark mass point [17, 22].

The light-quark mass dependence of the hadron masses is determined by chiral perturbation theory. There are non-analytic in m_q contributions from loop corrections which are calculable, as well as analytic terms which depend on low-energy constants (LECs) of the chiral Lagrangian. In the baryon sector, the leading non-analytic terms are $m_q^{3/2}$ and $m_q^2 \log m_q$. The $m_q^{3/2}$ term, which arises from Fig. 1 and is proportional to $M_{\pi,K,\eta}^3/(16\pi f^2)$ times axial couplings, is found to be rather large, naively of order a few hundred MeV. This term is absent for the pseudo-Goldstone boson masses, but is present for other mesons such as the vector mesons [23].

A surprising feature of recent lattice results is that the baryon masses as a function of $M_{\pi,K,\eta}$ do not show a large M^3 dependence. Fits to the baryon masses also give much smaller values for the baryon axial couplings, and require that the $M^3 \sim m_q^{3/2}$ term is almost completely cancelled by $m_q^2 \log m_q$ and m_q^2 terms. This cancellation must be accidental at the currently accessible lattice quark masses, since the terms have different m_q dependence. An alternative conclusion is that lattice quark masses are too large for $SU(3)$ chiral perturbation theory to be valid, and that perturbative chiral behavior sets in only for much smaller quark masses than the strange quark mass. This conclusion, however, fails to explain why $SU(3)$ flavor symmetry is so evident in baryon phenomenology.

The $1/N_c$ expansion constrains the structure of baryon chiral perturbation theory [4, 6, 9, 18]. Chiral corrections have to respect the spin-flavor structure of the $1/N_c$ expansion, and this leads to some important restrictions

¹ One inverse power of the quark mass is from the conjugate-gradient inversion of the fermion Dirac operator, which scales with the condition number. The additional inverse powers of the light quark mass arise from estimations of (i) the increased auto-correlation time of the HMC evolution as well as (ii) the molecular dynamics step-size used to adjust the acceptance rate. There are additional costs not counted here. For example, to keep the volume corrections exponentially small, one must work with $m_\pi L \gtrsim 4$, where L is the spatial size of the lattice.

on the form of the chiral loop corrections. For example, the baryon mass, which is of order N_c [2, 3], gets non-analytic corrections proportional to $m_s^{3/2}$, which are large. This large non-analytic contribution might lead one to expect that there should be large deviations from the Gell-Mann–Okubo mass relations, which were derived assuming that the mass operator was linear in m_s . One can show, however, that the $N_c m_s^{3/2}$ terms are a spin-flavor singlet, and give the same contribution to octet and decuplet baryons, whereas the $m_s^{3/2}$ terms are a spin-singlet flavor-octet, and the m_s^2/N_c terms are spin-singlet flavor-**27**. Only the latter terms contribute to the Gell-Mann–Okubo mass combinations, so that deviations from these relations are a factor of $1/N_c^2$ smaller than naive expectation and consistent with experiment. The small size of the Gell-Mann–Okubo relation was recently confirmed for a range of light quark masses [24]. For QCD, the cancellation to order $1/N_c^2$ arises as a numerical cancellation between octet and decuplet intermediate states [25]; to see the parametric form of the cancellation in $1/N_c$ requires computing the chiral corrections using the $SU(3)$ flavor representations of baryons containing N_c quarks.

The mass relations of Ref. [15] project the baryon masses onto different spin-flavor channels. By studying these mass relations as a function of m_q , one can investigate whether the unexpected chiral behavior arises in a particular channel.

The organization of this paper is as follows. In Section II, the baryon mass relations of the $1/N_c$ expansion are summarized briefly, and in Section III, the lattice simulation data are described. Section IV presents the results of a computation of $1/N_c$ mass combinations on the lattice for varying values of $SU(3)$ flavor symmetry breaking. Section V discusses the lattice analysis using heavy baryon chiral perturbation theory. Our conclusions are presented in Section VI.

II. $1/N_c$ BARYON MASS RELATIONS

The $1/N_c$ expansion of the baryon mass operator is²

$$\begin{aligned}
 H &= H^{1,0} + \epsilon H^{8,0} + \epsilon^2 H^{27,0} + \epsilon^3 H^{64,0}, \\
 H^{1,0} &= c_{(0)}^{1,0} N_c \mathbb{1} + c_{(2)}^{1,0} \frac{1}{N_c} J^2, \\
 H^{8,0} &= c_{(1)}^{8,0} T^8 + c_{(2)}^{8,0} \frac{1}{N_c} \{J^i, G^{i8}\} + c_{(3)}^{8,0} \frac{1}{N_c^2} \{J^2, T^8\}, \\
 H^{27,0} &= c_{(2)}^{27,0} \frac{1}{N_c} \{T^8, T^8\} + c_{(3)}^{27,0} \frac{1}{N_c^2} \{T^8, \{J^i, G^{i8}\}\}, \\
 H^{64,0} &= c_{(3)}^{64,0} \frac{1}{N_c^2} \{T^8, \{T^8, T^8\}\},
 \end{aligned} \tag{1}$$

² We use the notation and conventions of Ref [15].

where the superscript denotes the flavor- $SU(3)$ representation and the spin $SU(2)$ representation of each term. The parameter $\epsilon \propto m_s/\Lambda_\chi$ is a dimensionless measure of flavor- $SU(3)$ symmetry breaking. For the flavor **27** and **64** $1/N_c$ expansions, the operators on the r.h.s. are projected onto the corresponding $SU(3)$ flavor representations by subtracting out the lower-order representations, namely the singlet, octet, and, for the **64** $1/N_c$ expansion, the **27**. The coefficients $c_{(k)}^{i,j}$ are functions of $1/N_c$ and ϵ . The non-trivial content of the $1/N_c$ expansion is the $1/N_c$ suppression factors for the different terms in Eq. (1).

The $1/N_c$ expansion also holds at finite lattice spacing, so that an expansion of the form Eq. (1) is valid with coefficients that depend on the lattice spacing a .³ Thus the order N_c discretization correction is universal, and has the same value for all the octet and decuplet baryons. This term can be eliminated by studying baryon mass ratios or differences. The largest term that produces different discretization effects for the octet baryons is the T^8 term in $H^{8,0}$, which results in $\mathcal{O}(1)$ mass splittings that are $1/N_c$ suppressed relative to the leading mass term $N_c \mathbf{1}$.

The twelve $1/N_c$ mass relations that we study are tabulated in Table I. The eight mass relations M_1 – M_8 correspond to the first eight mass combinations in Table II of Ref. [15]. These mass relations are the mass combinations which occur at definite orders in $1/N_c$ and perturbative $SU(3)$ flavor symmetry breaking; each relation picks out a particular coefficient in Eq. (1). The mass combinations in Table I correspond to the coefficients listed in the table. There are two mass combinations, M_1 and M_2 , which are $SU(3)$ singlets and which occur at orders N_c and $1/N_c$, respectively. There are three flavor-octet mass combinations, M_3 , M_4 and M_5 , which are proportional to one factor of $SU(3)$ symmetry breaking ϵ and which occur at orders 1, $1/N_c$ and $1/N_c^2$, respectively. There are two flavor-**27** mass combinations, M_6 and M_7 , which occur at second order in $SU(3)$ breaking ϵ^2 and at orders $1/N_c$ and $1/N_c^2$ in the $1/N_c$ expansion. Finally, there is one mass combination M_8 which is suppressed by three powers of $SU(3)$ breaking ϵ^3 and by $1/N_c^2$ in the $1/N_c$ expansion. The additional four mass combinations M_A – M_D correspond to the first four mass relations of Ref. [6]. These baryon mass combinations are each order $1/N_c^2$ in the $1/N_c$ expansion. The mass relations were derived assuming only isospin symmetry. Thus, these relations do not assume approximate $SU(3)$ flavor symmetry and are valid even for very large $SU(3)$ flavor symmetry breaking. Only three of the four combinations M_A – M_D are linearly independent.

Each mass relation defines a mass combination of the

octet and decuplet masses M_i of the form

$$\mathbf{M} = \sum_i c_i M_i. \quad (2)$$

In this work, isospin breaking is neglected, so each M_i denotes the average mass of a baryon isomultiplet. The normalization of each mass relation is arbitrary, and depends on a particular choice of normalization for coefficients in the Hamiltonian, i.e. $c_i \rightarrow \lambda c_i$ defines another mass relation with the same spin-flavor quantum numbers. To remove the rescaling ambiguity, Ref. [15] used the accuracy

$$A \equiv \frac{\sum_i c_i M_i}{\frac{1}{2} \sum_i |c_i| M_i}. \quad (3)$$

to quantify the fractional error of a given mass relation. Here we use a related quantity, the scale invariant mass combination

$$R \equiv \frac{\sum_i c_i M_i}{\sum_i |c_i|}. \quad (4)$$

Dividing by $\sum_i |c_i|$ instead of by $\frac{1}{2} \sum_i |c_i| M_i$ avoids mixing different spin-flavor representations via the denominator factor. The rescaled relations R_{1-8} and R_{A-D} have dimensions of mass.

In our numerical analysis, we shall use the dimensionless variable

$$\epsilon = \frac{M_K^2 - M_\pi^2}{\Lambda_\chi^2} \quad (5)$$

as a measure of $SU(3)$ breaking, where $\Lambda_\chi \sim 4\pi f \approx 1$ GeV [26] is the scale of chiral symmetry breaking.

III. LATTICE SIMULATION

In this work, we use the results of the recent LHPC spectrum calculation [27] to explore the mass combinations of the $1/N_c$ expansion. The LHP Collaboration utilized a mixed-action lattice calculation with domain-wall [28–30] valence propagators computed with the Asqtad improved [31, 32] dynamical MILC gauge ensembles [33, 34].⁴ The calculation was performed at one lattice spacing with $a \sim 0.125$ fm, and a fixed spatial volume $L \sim 2.5$ fm. The pion and kaon masses used in Ref. [27] are $\{M_\pi, M_K\} = \{293, 586\}$, $\{356, 604\}$, $\{496, 647\}$, $\{597, 686\}$, $\{689, 729\}$ and $\{758, 758\}$ MeV, respectively, on the m007, m010, m020, m030, m040, and m050 ensembles, where the labels denote the light quark masses in lattice units.⁵ In the dynamical ensembles and

³ Rotational symmetry is broken down to a discrete cubic symmetry, so that spin is replaced by irreducible representations of the cubic group.

⁴ The strange quark and many of the light quark propagators were computed by the NPLQCD Collaboration [35].

⁵ The mass M_η is defined at this order by the Gell-Mann–Okubo formula $M_\eta^2 = \frac{4}{3} M_K^2 - \frac{1}{3} M_\pi^2$.

TABLE I: Mass combinations M_1 – M_8 from Ref. [15] and M_A – M_D from Ref. [6]. The coefficients and orders in $1/N_c$ and perturbative $SU(3)$ flavor symmetry breaking ϵ are given for mass combinations M_1 – M_8 . Combinations M_A – M_D are obtained at order $1/N_c^2$ assuming only isospin flavor symmetry.

Label	Operator	Coefficient	Mass Combination	$1/N_c$	$SU(3)$
M_1	$\mathbb{1}$	$160 N_c c_{(0)}^{1,0}$	$25(2N + \Lambda + 3\Sigma + 2\Xi) - 4(4\Delta + 3\Sigma^* + 2\Xi^* + \Omega)$	N_c	1
M_2	J^2	$-120 \frac{1}{N_c} c_{(2)}^{1,0}$	$5(2N + \Lambda + 3\Sigma + 2\Xi) - 4(4\Delta + 3\Sigma^* + 2\Xi^* + \Omega)$	$1/N_c$	1
M_3	T^8	$20\sqrt{3} \epsilon c_{(1)}^{8,0}$	$5(6N + \Lambda - 3\Sigma - 4\Xi) - 2(2\Delta - \Xi^* - \Omega)$	1	ϵ
M_4	$\{J^i, G^{i8}\}$	$-5\sqrt{3} \frac{1}{N_c} \epsilon c_{(2)}^{8,0}$	$N + \Lambda - 3\Sigma + \Xi$	$1/N_c$	ϵ
M_5	$\{J^2, T^8\}$	$30\sqrt{3} \frac{1}{N_c^2} \epsilon c_{(3)}^{8,0}$	$(-2N + 3\Lambda - 9\Sigma + 8\Xi) + 2(2\Delta - \Xi^* - \Omega)$	$1/N_c^2$	ϵ
M_6	$\{T^8, T^8\}$	$126 \frac{1}{N_c} \epsilon^2 c_{(2)}^{27,0}$	$35(2N - 3\Lambda - \Sigma + 2\Xi) - 4(4\Delta - 5\Sigma^* - 2\Xi^* + 3\Omega)$	$1/N_c$	ϵ^2
M_7	$\{T^8, J^i G^{i8}\}$	$-63 \frac{1}{N_c^2} \epsilon^2 c_{(3)}^{27,0}$	$7(2N - 3\Lambda - \Sigma + 2\Xi) - 2(4\Delta - 5\Sigma^* - 2\Xi^* + 3\Omega)$	$1/N_c^2$	ϵ^2
M_8	$\{T^8, \{T^8, T^8\}\}$	$9\sqrt{3} \frac{1}{N_c^3} \epsilon^3 c_{(3)}^{64,0}$	$\Delta - 3\Sigma^* + 3\Xi^* - \Omega$	$1/N_c^3$	ϵ^3
M_A			$(\Sigma^* - \Sigma) - (\Xi^* - \Xi)$	$1/N_c^2$	–
M_B			$\frac{1}{3} (\Sigma + 2\Sigma^*) - \Lambda - \frac{2}{3} (\Delta - N)$	$1/N_c^2$	–
M_C			$-\frac{1}{4} (2N - 3\Lambda - \Sigma + 2\Xi) + \frac{1}{4} (\Delta - \Sigma^* - \Xi^* + \Omega)$	$1/N_c^2$	–
M_D			$-\frac{1}{2} (\Delta - 3\Sigma^* + 3\Xi^* - \Omega)$	$1/N_c^2$	–

the computation of the valence propagators, the strange quark was held fixed near its physical value. (In fact the strange quark was $\sim 25\%$ too large [36].) For further details of the calculation, we refer the reader to Ref. [27].

Using the *bootstrap resampled* lattice data, we determine the 12 mass combinations of Table I on each ensemble. The results are collected in Table II. These results were determined with the absolute scale of $a^{-1} = 1588$ MeV on all coarse ensembles, where this scale used in Ref. [27] was determined from heavy quark spectroscopy. We have additionally determined the mass combinations using the smoothed values of r_1/a , where r_1 is determined on each different ensemble from the heavy quark potential with $r_1^2 F(r_1) = 1$ [37]. The values of a^{-1} determined in this way range from $\{1597, 1590, 1614, 1621, 1628, 1634\}$ MeV from the lightest to heaviest quark mass. These two scale-setting methods are in good agreement, as shown in the next section.

IV. COMPARISON WITH LATTICE DATA

A plot of the lattice baryon masses as a function of M_π is given in Fig. 2. The triangles are the lattice data, and the blue squares are the Particle Data Group (PDG) values.⁶ The usual way of studying the data is to fit to the individual baryon masses. The $1/N_c$ analysis shows that

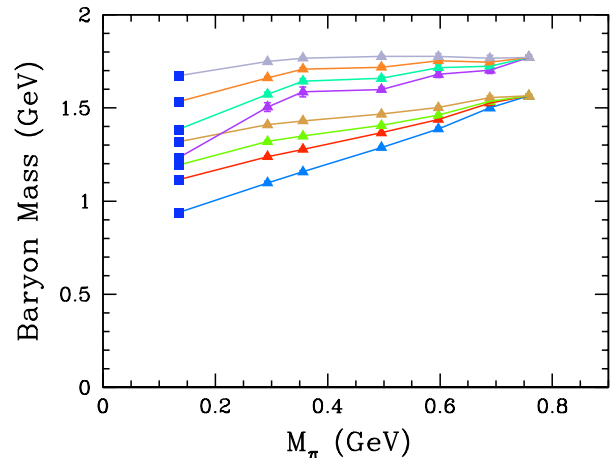


FIG. 2: Octet and decuplet baryon lattice masses as a function of M_π . The blue squares are the PDG values and the triangles are lattice data of the LHP Collaboration simulated with fixed m_s and varying m_{ud} . The two right-most points simulate the flavor-singlet baryon masses in the exact $SU(3)$ flavor symmetry limit $M_\pi = M_K$. The (PDG) baryons from bottom to top are $N, \Lambda, \Sigma, \Delta, \Xi, \Sigma^*, \Xi^*, \Omega$.

a more useful approach is to instead study the mass combinations in Table I, as these combinations have definite $1/N_c$ and $SU(3)$ scaling properties.

In this section, we present a series of plots of the 12 scale invariant baryon mass combinations (see Eq. (4)) R_1 – R_8 and R_A – R_D as a function of $SU(3)$ flavor symmetry breaking. In each plot, the red triangles and green circles

⁶ Note that M_K varies slightly for the different M_π values and is not exactly equal to the physical M_K .

TABLE II: Values of mass combinations M_i in GeV using the scale setting $a^{-1} = 1.588$ GeV.

$M_K^2 - M_\pi^2 [\text{GeV}^2]$	0.2579	0.2380	0.1718	0.1141	0.0574	0
$M_1 [\text{GeV}]$	192(1)	197(1)	211(1)	221(2)	237(2)	242(1)
$M_2 [\text{GeV}]$	-12.2(5)	-13.3(6)	-10.9(4)	-10.6(6)	-7.8(6)	-8.2(4)
$M_3 [\text{GeV}]$	-8.07(20)	-7.15(15)	-4.40(08)	-2.81(09)	-1.28(04)	0
$M_4 [\text{GeV}]$	-0.214(10)	-0.181(7)	-0.099(5)	-0.056(6)	-0.022(3)	0
$M_5 [\text{GeV}]$	0.29(7)	0.35(8)	0.13(3)	0.14(5)	0.04(2)	0
$M_6 [\text{GeV}]$	-1.05(36)	-0.25(26)	-0.003(71)	0.15(14)	-0.02(1)	0
$M_7 [\text{GeV}]$	-0.30(12)	-0.05(11)	0.005(24)	0.08(7)	-0.003(4)	0
$M_8 [\text{GeV}]$	0.02(1)	0.012(09)	-0.001(1)	0.015(12)	0.00004(6)	0
$M_A [\text{GeV}]$	0.0004(58)	0.018(7)	0.001(3)	0.004(4)	-0.0003(19)	0
$M_B [\text{GeV}]$	-0.022(10)	-0.018(10)	-0.0004(30)	-0.003(3)	0.0000(13)	0
$M_C [\text{GeV}]$	0.010(4)	0.002(4)	-0.0002(8)	-0.003(3)	0.0001(1)	0
$M_D [\text{GeV}]$	-0.012(5)	-0.0061(45)	0.0004(6)	-0.0076(58)	-0.00002(3)	0

cles are the lattice data, and the errors on the mass combination have been computed using the *bootstrap* data sets of the octet and decuplet masses, taking advantage of the full correlations in the lattice data. The red triangles and green circles are the lattice results using the two different scale-setting methods. The red points are determined with the absolute scale setting $a^{-1} = 1588$ MeV, and the green points are determined with the smoothed r_1/a values [37]. The blue square is obtained using the physical baryon and meson masses from the PDG [38], with the error bar computed using experimental uncertainties on the isospin averaged masses. For most of the plots, the error on the blue point is smaller than size of the point, and is not visible.

The horizontal axis is $M_K^2 - M_\pi^2$ in units of $(\text{GeV})^2$, which is a measure of $SU(3)$ flavor symmetry breaking, and the vertical axis is the mass combination in MeV. For mass combinations proportional to powers of $SU(3)$ breaking, we plot both the mass combination and the mass combination divided by the appropriate power of ϵ , using the definition Eq. (5) for ϵ , so that the units remain MeV.

The average $O(N_c)$ mass of the octet and decuplet baryons is ~ 1300 MeV. Naive power counting with $N_c = 3$ implies order N_c masses are ~ 1300 MeV, order 1 masses are ~ 430 MeV, order $1/N_c$ masses are ~ 140 MeV, order $1/N_c^2$ masses are ~ 50 MeV, and order $1/N_c^3$ masses are ~ 15 MeV. This $1/N_c$ hierarchy is evident in the baryon masses R_1 - R_8 and R_A - R_D below.

Fig. 3 plots the first relation R_1 which corresponds to the $N_c \mathbb{1}$ operator in the $1/N_c$ expansion. This operator is order 1 GeV and is seen to be fairly independent of $SU(3)$ breaking. The deviation of the physical point from the lattice data is presumably due to the larger than physical strange quark mass. In principle, this relation is also susceptible to finite discretization errors, beginning at $\mathcal{O}(a^2)$, although these are expected to be small for this

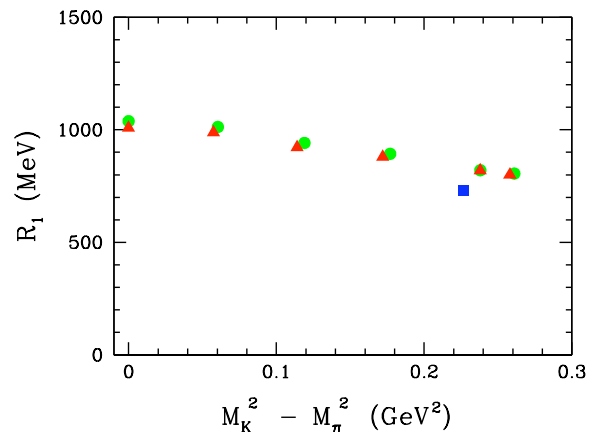


FIG. 3: R_1 as a function of $(M_K^2 - M_\pi^2)$. The red triangles and green circles are lattice results with two different scale setting methods (see text), and the blue square is using the PDG values for the hadron masses.

data set [27].

Fig. 4 plots the second relation R_2 , which corresponds to the J^2/N_c operator in the $1/N_c$ expansion. This hyperfine splitting is predicted to be order $1/N_c$, and so of order 140 MeV. The mass combination R_2 is clearly suppressed relative to the average ground state baryon mass R_1 . The lattice results allow us to study this mass combination as a function of $SU(3)$ breaking. Notice that the relation works independently of $SU(3)$ breaking, and that R_2 does not vanish at the $SU(3)$ symmetry point $M_K^2 = M_\pi^2$. The numerical results clearly show that the suppression of R_2 is a consequence of $1/N_c$, and not due to a hidden flavor breaking suppression factor.

Fig. 5 plots the third relation R_3 , which is of order ϵ . The relation vanishes as $M_K^2 - M_\pi^2 \rightarrow 0$, as can be seen in the upper panel. The lower panel divides the mass

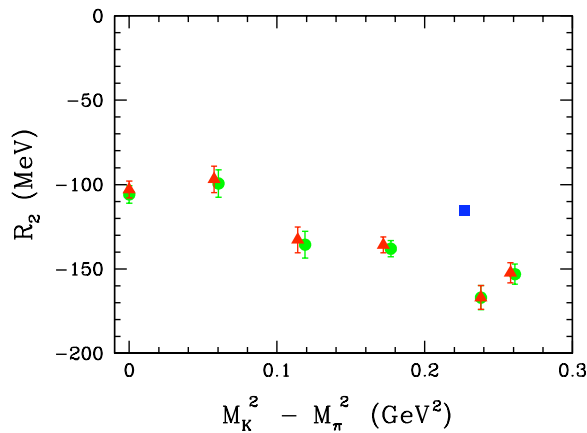


FIG. 4: R_2 as a function of $(M_K^2 - M_\pi^2)$. The red triangles and green circles are lattice results with two different scale setting methods (see text), and the blue square is using the PDG values for the hadron masses.

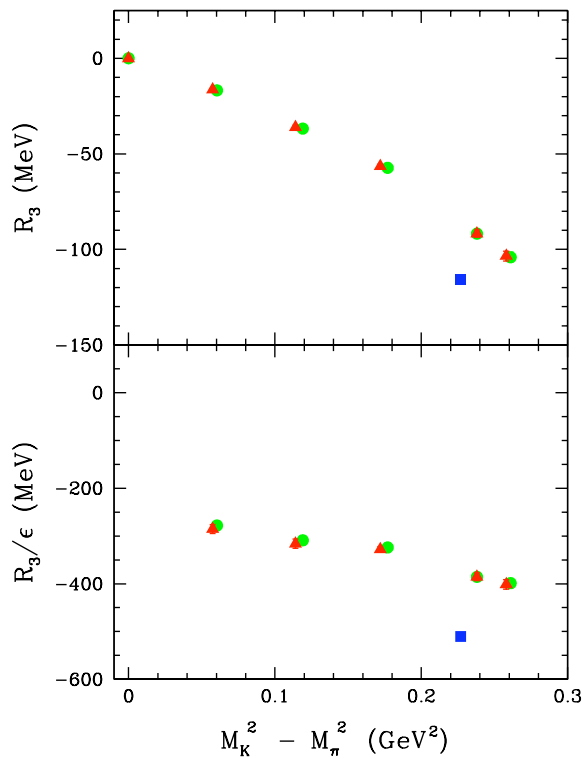


FIG. 5: R_3 and R_3/ϵ as a function of $(M_K^2 - M_\pi^2)$.

relation by ϵ , and shows that R_3/ϵ is $O(1)$ in the $1/N_c$ expansion, as expected. Notice that R_3/ϵ does not vanish in the $SU(3)$ symmetry limit. The $SU(3)$ symmetry point of the lattice data is omitted in the R_3/ϵ plot, as it involves dividing by zero.

Fig. 6 plots R_4 and R_4/ϵ , which are of order ϵ/N_c and $1/N_c$, respectively. The mass combinations R_3 and R_4 are both order ϵ , but R_4 is suppressed relative to R_3 by an additional factor of $1/N_c$. This suppression is clearly

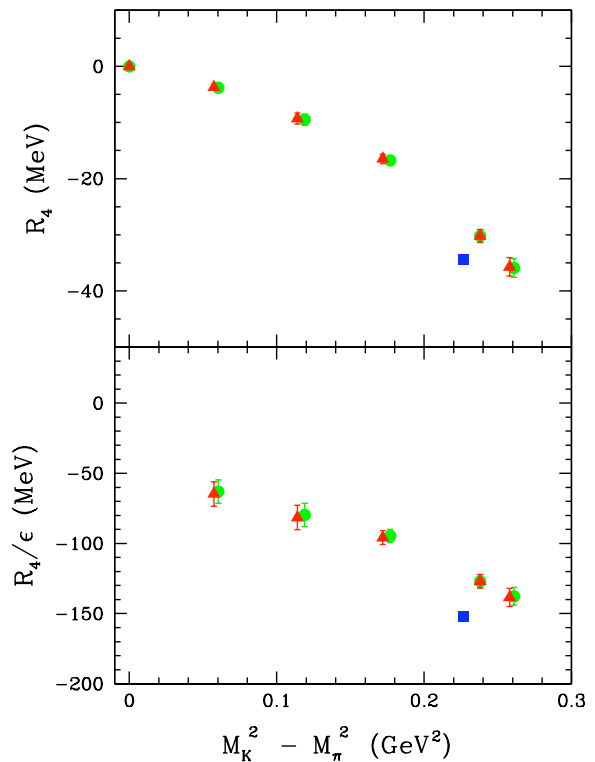


FIG. 6: R_4 and R_4/ϵ as a function of $(M_K^2 - M_\pi^2)$.

visible in the numerical values. R_4 is seen to vanish in the $SU(3)$ symmetry limit. Again, R_4/ϵ does not vanish at the $SU(3)$ symmetric point. Both R_3/ϵ and R_4/ϵ display some dependence on $SU(3)$ symmetry breaking, which implies that there is ϵ dependence in the coefficients $c_{(1)}^{8,0}$ and $c_{(2)}^{8,0}$, respectively.

Fig. 7 plots R_5 and R_5/ϵ , which are of order ϵ/N_c^2 and $1/N_c^2$, respectively. The mass combinations are of the expected size, but the lattice data points now have relatively large errors.

R_{6-8} are plotted in Figs. 8–10, respectively, for completeness. In each case, the physical point (blue square) has the expected size, and the lattice results are compatible with $1/N_c$ and ϵ power counting expectations, but the error bars are now rather large.

The last four plots, Figs. 11–14, are the first four relations in the introduction of Ref. [6], which were derived without assuming $SU(3)$ symmetry, and are of order $1/N_c^2$. They are listed as $M_A - M_D$ in Table I. From the plots, it is evident that $R_A - R_D$ are satisfied irrespective of the value of $SU(3)$ breaking. It would be interesting to see how well these relations work at even *larger* values of $SU(3)$ breaking. The relation M_A in the limit $m_s \rightarrow \infty$ goes over into the mass relation for heavy quark baryons, $\Sigma_Q^* - \Sigma_Q = \Xi_Q^* - \Xi_Q'$, so it would be interesting to look at the cross-over to heavy quark behavior in which the hyperfine splitting becomes proportional to $1/m_Q$.

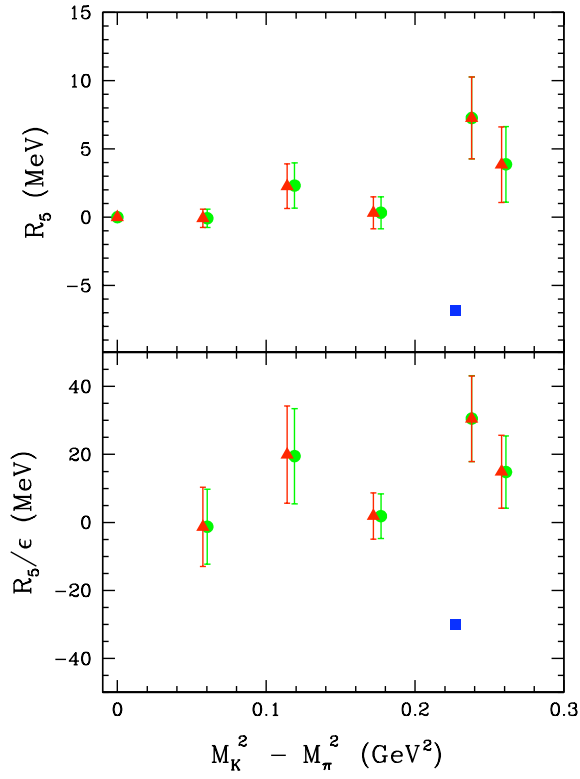


FIG. 7: R_5 and R_5/ϵ as a function of $(M_K^2 - M_\pi^2)$.

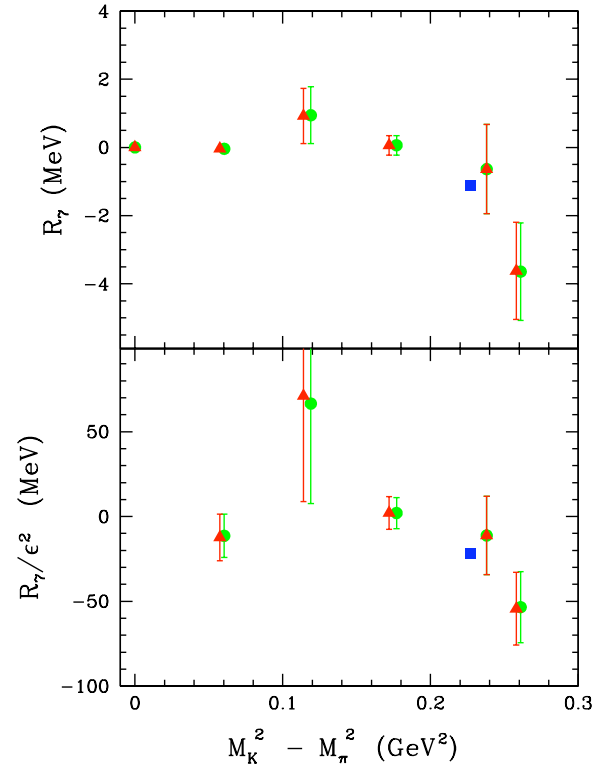


FIG. 9: R_7 and R_7/ϵ^2 as a function of $(M_K^2 - M_\pi^2)$.

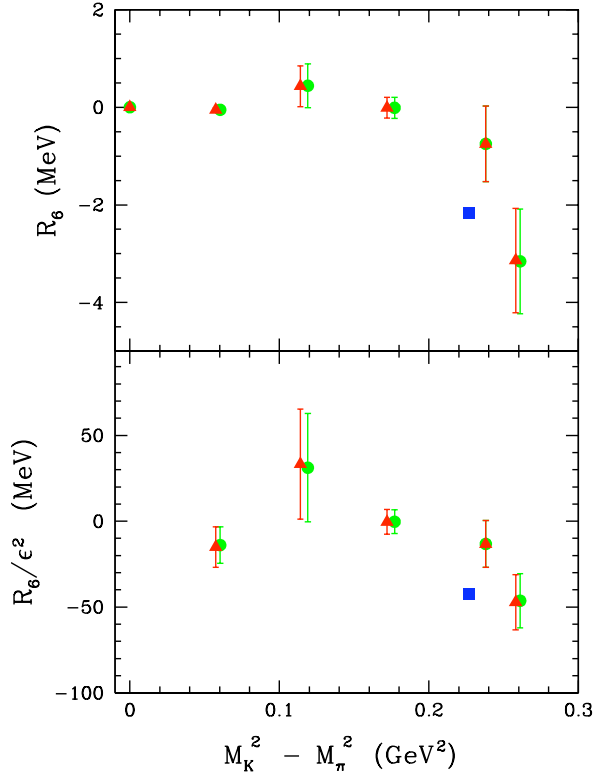


FIG. 8: R_6 and R_6/ϵ^2 as a function of $(M_K^2 - M_\pi^2)$.

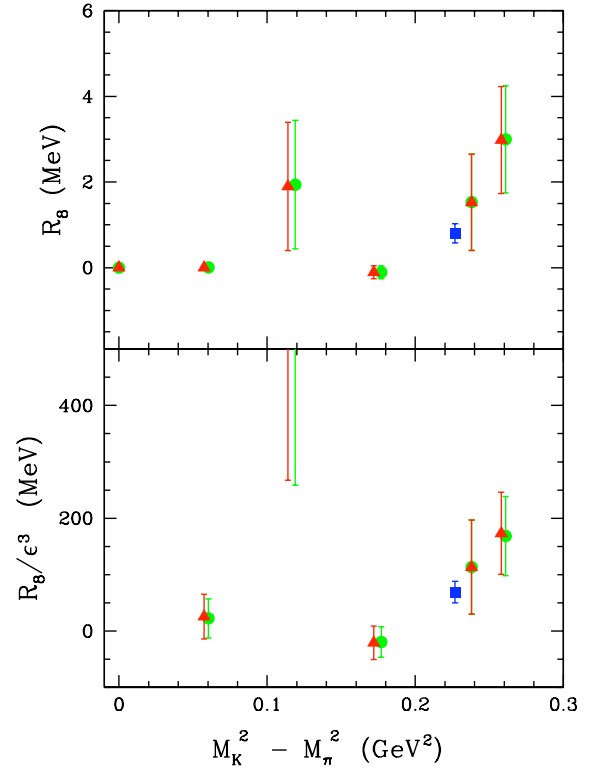
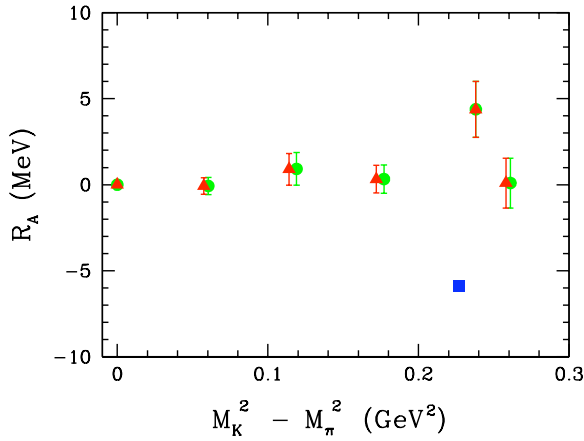
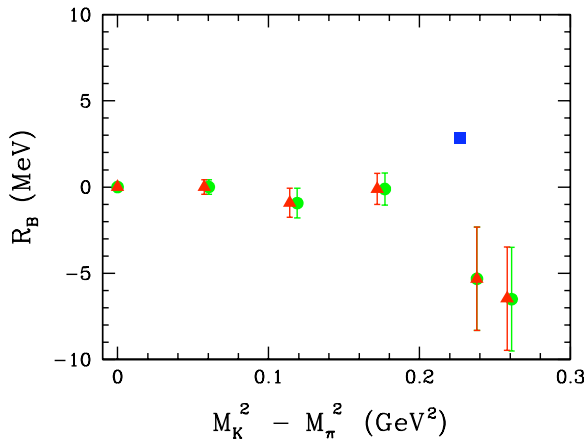


FIG. 10: R_8 and R_8/ϵ^3 as a function of $(M_K^2 - M_\pi^2)$.

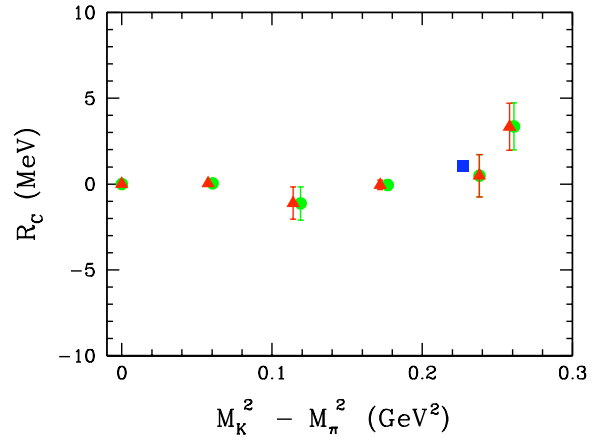
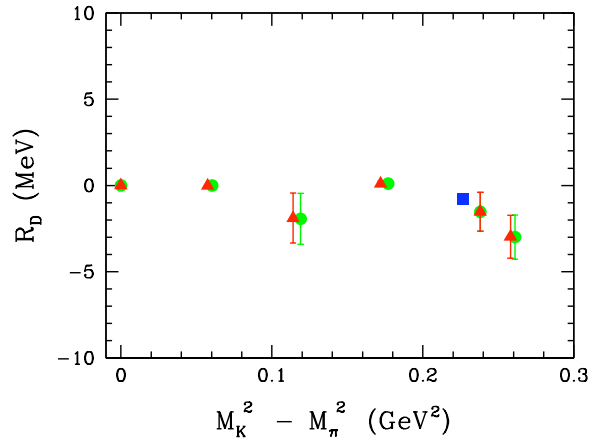
FIG. 11: R_A as a function of $(M_K^2 - M_\pi^2)$.FIG. 12: R_B as a function of $(M_K^2 - M_\pi^2)$.

V. HEAVY BARYON χ PT ANALYSIS

To compare these lattice mass combinations directly with the experimental values, we must extrapolate them to the physical point. The light and strange quark mass dependence is described by $SU(3)$ heavy baryon chiral perturbation theory (HB χ PT) [25]. The baryon chiral Lagrangian is given by

$$\begin{aligned} \mathcal{L} = & \text{Tr}(\bar{B}i v \cdot DB) - \bar{T}^\mu [i v \cdot D - \Delta_0] T_\mu \\ & + b_D \text{Tr}(\bar{B}\{\mathcal{M}_+, B\}) + b_F \text{Tr}(\bar{B}[\mathcal{M}_+, B]) \\ & + b_0 \text{Tr}(\bar{B}B) \text{Tr}(\mathcal{M}_+) \\ & + \gamma_M \bar{T}^\mu \mathcal{M}_+ T_\mu - \bar{\sigma} \bar{T}^\mu T_\mu \text{Tr}(\mathcal{M}_+) \\ & + 2D \text{Tr}(\bar{B}S^\mu \{\mathcal{A}_\mu, B\}) + 2F \text{Tr}(\bar{B}S^\mu [\mathcal{A}_\mu, B]) \\ & + 2\mathcal{H} \bar{T}^\mu S_\nu \mathcal{A}^\nu T_\mu + \mathcal{C} (\bar{T}^\mu \mathcal{A}_\mu B + \bar{B} \mathcal{A}_\mu T^\mu). \end{aligned} \quad (6)$$

where B and T_μ are the octet and decuplet fields, respectively; v is the four velocity of the baryon and S_μ is the spin-vector. The decuplet–octet mass splitting in the chiral limit is Δ_0 , and \mathcal{M}_+ is the mass spurion defined

FIG. 13: R_C as a function of $(M_K^2 - M_\pi^2)$.FIG. 14: R_D as a function of $(M_K^2 - M_\pi^2)$.

by

$$\mathcal{M}_+ = \xi^\dagger m_Q \xi^\dagger + \xi m_Q^\dagger \xi \quad (7)$$

in terms of the light quark mass matrix

$$m_Q = \begin{pmatrix} m_u & & \\ & m_d & \\ & & m_s \end{pmatrix}, \quad (8)$$

and $\xi = e^{i\Pi/f_\pi}$. The covariant derivative is

$$D_\mu B = \partial_\mu B + [\mathcal{V}_\mu, B], \quad (9)$$

and the vector and axial fields are

$$\mathcal{V}_\mu = \frac{1}{2} (\xi \partial_\mu \xi^\dagger + \xi^\dagger \partial_\mu \xi), \quad (10)$$

$$\mathcal{A}_\mu = \frac{i}{2} (\xi \partial_\mu \xi^\dagger - \xi^\dagger \partial_\mu \xi). \quad (11)$$

The masses of the octet and decuplet baryons were first determined in Ref. [39] to next-to leading order (NLO), $\mathcal{O}(M_{K,\pi}^3)$. The octet baryon masses were later

determined to next-to-next-to leading order (NNLO), $\mathcal{O}(M_{K,\pi}^4)$ in Refs. [40–42], and the decuplet baryons to NNLO in Refs. [43, 44].

The lattice calculation of baryon masses used for this work was a mixed-action calculation [27]. Therefore, the calculation, and corresponding low-energy effective field theory for the baryons is inherently partially quenched. The partially quenched Lagrangian for heavy baryons was determined by Chen and Savage [45] through NLO. The extension of the partially quenched Lagrangian to the mixed-action Lagrangian, which includes corrections from the lattice spacing, is also known [46, 47], through NNLO [42, 44, 47]. At NLO, the corrections from the mixed action are straightforward, amounting to corrections to the mixed valence-sea meson masses [48] appearing in the one-loop self-energy corrections, Fig. 1, as well as the partially quenched hairpin corrections [45]. A rigorous extrapolation to the continuum limit requires multiple lattice spacings, but the lattice data used in this work was performed at a single lattice spacing (albeit with the size of the discretization corrections expected to be small, see Ref. [27] for details). However, one can make a qualitative estimate of the size of the discretization errors by comparing the extrapolations performed with the continuum extrapolation formulae and the mixed-action formulae. We now perform these chiral extrapolations.

A. Variable projected χ^2 minimization

To perform the minimization, we use the *bootstrap resampled* lattice data to form the covariance matrix,

$$C_{q,q'} = \frac{1}{N_{bs}} \sum_{bs}^{N_{bs}} \left(M_q[bs] - \bar{M}_q \right) \left(M_{q'}[bs] - \bar{M}_{q'} \right), \quad (12)$$

where q is a super-mass index which runs over both the mass relations M_1 – M_7 as well as the different lattice ensembles m007–m050. We then construct the χ^2 ,

$$\chi^2 = \sum_{q,q'} \left(\bar{M}_q - f(M_q, \lambda) \right) C_{q,q'}^{-1} \left(\bar{M}_{q'} - f(M_{q'}, \lambda) \right), \quad (13)$$

where $f(M_q, \lambda)$ is the HB χ PT extrapolation formula for the mass relation M_q and depends upon the low-energy constants $\vec{\lambda} \equiv \{M_0, \Delta_0, b_D, b_F, b_0, \bar{\sigma}, \gamma_M, D, F, \mathcal{C}, \mathcal{H}, \dots\}$. At NLO, the baryon mass extrapolation formulae are linearly dependent upon all the λ_i , except for D and F (they are linearly dependent upon \mathcal{C}^2 and \mathcal{H}^2). Therefore, to perform the numerical minimization, we first perform a linear least squares fit on all the linear LECs, $\vec{\lambda}_{lin.} \equiv \{M_0, \Delta_0, b_D, b_F, b_0, \bar{\sigma}, \gamma_M, \mathcal{C}^2, \mathcal{H}^2\}$, solving for these low-energy constants as functions of D and F , and then perform the numerical minimization. This is known as the variable projection (VarPro) method [49].

We first perform the χ^2 minimization using relations M_1 – M_7 and the NLO extrapolation formulae.⁷ In Tables III and IV, we collect the results of both the continuum extrapolation and the mixed-action extrapolation. In these tables, the partially quenched/mixed-action low-energy constants $\alpha_M, \beta_M, \sigma_M, \gamma_M$ and $\bar{\sigma}_M$ are related to the LECs of $SU(3)$ HB χ PT of Eq. (6) by

$$b_D = \frac{1}{4} (\alpha_M - 2\beta_M), \quad \gamma_M = \gamma_M^{(PQ)}, \quad (14)$$

$$b_F = \frac{1}{2} (5\alpha_M + 2\beta_M), \quad \bar{\sigma}_M = \bar{\sigma}_M^{(PQ)}, \quad (15)$$

$$b_0 = \sigma_M + \frac{1}{6}\alpha_M + \frac{2}{3}\beta_M. \quad (16)$$

Then, for example, $\tilde{\alpha}_M = \alpha_M/B_0$ where at leading order $M_K^2 = B_0(m_s + m_{ud})$. In both cases, we perform the fit for four different ranges of the quark masses. The first fit includes only the lightest two mass points, while each successive fit includes an additional mass point. The results of the mixed action and continuum fits are fairly consistent, as can be seen in Tables III and IV.

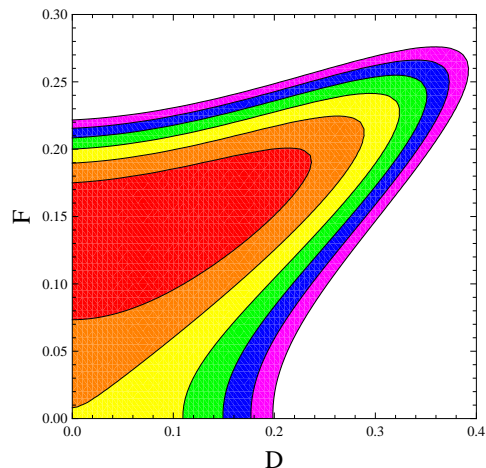


FIG. 15: Continuum HB χ PT χ^2 as a function of D and F from the m007–m010 minimization. The n^{th} contour satisfies $\chi^2 = \chi_{min}^2 + n$.

Consistent with Ref. [27], we find the values of D and F are significantly smaller than those determined either phenomenologically [50] or with the recent lattice determination [51] (these determinations provide $D \simeq 0.72$ and $F \simeq 0.45$). With the use of the VarPro method, we have reduced the numerical minimization to a 2-dimensional problem, thus allowing us to plot the resulting χ^2 as a function of D and F . In Fig. 15, we plot the resulting χ^2 for the continuum fit using the lightest two

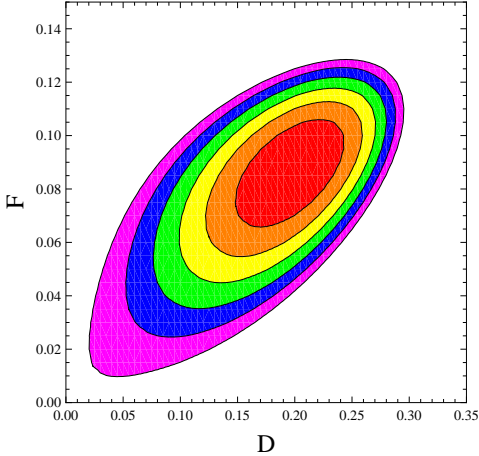
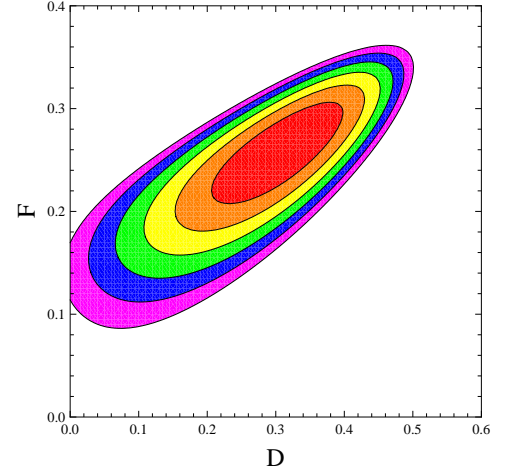
⁷ The mass relation M_8 is in fact exactly zero through NNLO. In the partially quenched theory, this mass relation exactly vanishes at NLO, and at NNLO, there are residual partially quenched effects which do not exactly cancel [44].

TABLE III: Fit to Mass Relations R_1 – R_7 using NLO continuum HB χ PT with a variation projection (VarPro) method.

Fit Range	D	F	M_0	Δ_0	$\tilde{\alpha}_M$	$\tilde{\beta}_M$	$\tilde{\gamma}_M$	$\tilde{\sigma}$	$\tilde{\bar{\sigma}}$	C^2	H^2
			[GeV]	[GeV]	[GeV] $^{-1}$	[GeV] $^{-1}$	[GeV] $^{-1}$	[GeV] $^{-1}$	[GeV] $^{-1}$		
m007 – m010	0.04(28)	0.14(6)	0.999(49)	0.21(16)	–0.58(7)	–0.42(16)	0.68(37)	–0.10(6)	–0.36(31)	0.01(12)	0.32(55)
m007 – m020	0.17(8)	0.07(5)	0.972(18)	0.48(5)	–0.67(2)	–0.81(5)	0.39(12)	–0.11(2)	0.09(9)	0.21(3)	0.09(19)
m007 – m030	0.21(5)	0.08(3)	0.972(13)	0.44(5)	–0.67(2)	–0.76(3)	0.49(12)	–0.12(1)	–0.00(8)	0.15(2)	0.18(18)
m007 – m040	0.20(5)	0.09(2)	0.960(11)	0.43(04)	–0.67(1)	–0.73(3)	0.62(8)	–0.13(1)	–0.05(6)	0.14(2)	0.35(13)

TABLE IV: Fit to Mass Relations R_1 – R_7 using NLO mixed action HB χ PT with a variation projection (VarPro) method.

Fit Range	D	F	M_0	Δ_0	$\tilde{\alpha}_M$	$\tilde{\beta}_M$	$\tilde{\gamma}_M$	$\tilde{\sigma}$	$\tilde{\bar{\sigma}}$	C^2	H^2
			[GeV]	[GeV]	[GeV] $^{-1}$	[GeV] $^{-1}$	[GeV] $^{-1}$	[GeV] $^{-1}$	[GeV] $^{-1}$		
m007 – m010	0.31(9)	0.26(5)	0.941(42)	0.242(73)	–1.29(1)	–0.46(1)	3.8(9)	–0.35(5)	–1.8(4)	–0.043(9)	4.3(1.1)
m007 – m020	0.36(3)	0.19(2)	0.989(15)	0.365(30)	–1.03(1)	–0.70(1)	0.66(22)	–0.24(2)	–0.22(11)	–0.009(4)	0.21(26)
m007 – m030	0.35(2)	0.16(2)	1.001(11)	0.368(28)	–0.92(1)	–0.71(1)	0.58(21)	–0.20(1)	–0.15(10)	–0.007(4)	0.11(25)
m007 – m040	0.34(2)	0.15(1)	0.995(8)	0.376(26)	–0.87(1)	–0.70(1)	0.69(18)	–0.20(1)	–0.16(8)	–0.001(2)	0.21(21)

FIG. 16: Continuum HB χ PT χ^2 as a function of D and F from the m007–m040 minimization.FIG. 17: Mixed action HB χ PT χ^2 as a function of D and F from the m007–m010 minimization. The n^{th} contour satisfies $\chi^2 = \chi_{\text{min}}^2 + n$.

ensembles. In Fig. 16, we plot the resulting χ^2 for the continuum extrapolation using the lightest five ensembles. Figs. 17 and 18 display the same plots constructed with the mixed action extrapolation formulae.

One observes the mixed action analysis returns values of D and F which are slightly larger than from the $SU(3)$ analysis, but still smaller than expected. In Table V, we use the resulting LECs from the continuum analysis to compare with the experimental values of both the baryon masses as well as with the mass combinations in Table I (within a few sigma, the mixed action extrapolations are consistent). Despite the apparent discrepancy in the values of D and F , one observes the extrapolated values of

both the baryon masses and the mass combinations, measured as a percent deviation, are in reasonable agreement with experiment.

We caution that one can not draw strong conclusions about $SU(3)$ HB χ PT from this analysis, in particular the small values of D and F . First, the values of $M_{K,\pi}$ used in this work are still larger than desirable for performing chiral extrapolations (in fact the strange quark mass is known to be $\sim 25\%$ too heavy [36]). Second, at NLO, the baryon masses are predicted to have large $M_{K,\pi}^3$ corrections, however, this is not observed in the numerical results for the baryon masses themselves, see Fig. 2. This

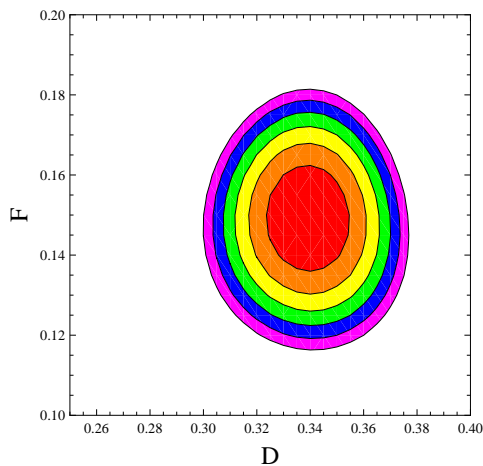


FIG. 18: Mixed action HB χ PT χ^2 as a function of D and F from the m007–m040 minimization.

TABLE V: Predicted baryon masses and mass relations from fit in Tab. III. The predicted values are listed according to the heaviest light quark mass used. The m030 fit is consistent with that of m020 and m040.

M_i	Exp. [GeV]	m010 [GeV]	m020 [GeV]	m040 [GeV]
M_N	0.939	1.039(31)	1.023(12)	1.020(8)
M_Λ	1.116	1.159(22)	1.145(9)	1.142(6)
M_Σ	1.193	1.219(22)	1.231(9)	1.221(7)
M_Ξ	1.318	1.306(16)	1.309(7)	1.303(5)
M_Δ	1.232	1.376(30)	1.454(12)	1.427(9)
M_{Σ^*}	1.385	1.461(28)	1.531(10)	1.516(8)
M_{Ξ^*}	1.533	1.543(27)	1.600(10)	1.598(7)
M_Ω	1.672	1.622(27)	1.663(9)	1.672(6)
M_1	175	179(4)	176(2)	176(1)
M_2	-9.2	-11(1)	-13.6(4)	-13.2(3)
M_3	-9.03	-6.6(6)	-7.5(2)	-7.2(1)
M_4	-0.21	-0.15(1)	-0.22(1)	-0.20(1)
M_5	-0.21	0.05(12)	0.07(5)	-0.00(4)
M_6	-0.73	-0.12(14)	0.17(7)	0.22(4)
M_7	-0.092	0.01(3)	0.09(1)	0.109(9)
M_A	-0.024	0.00(1)	0.009(5)	0.001(4)
M_B	0.0097	-0.003(8)	-0.001(4)	0.004(3)
M_C	0.0031	-0.000(1)	-0.0033(5)	-0.0039(3)

means there must be strong cancellation between the different orders in the chiral expansion to produce the observed results.⁸ In order for the chiral extrapolation analysis to be consistent with both the baryon masses and the expected values of D and F , one may need to use lighter

⁸ In the case of the nucleon, the cancellation is such that the mass is well described by a fit function linear in M_π [52].

quark masses and to include $\mathcal{O}(M_{K,\pi}^4)$ contributions to the masses. Further, it is likely that a combined analysis of both the masses and the axial couplings will be required.

Performing the complete NNLO analysis of the octet and decuplet baryon masses introduces 19 new unknown LECs (for 30 total). Twelve of these LECs correspond to $\mathcal{O}(m_q^2)$ operators of the form $\text{Tr}(\bar{B}\mathcal{M}_+\mathcal{M}_+B)$ and give rise to $M_{\pi,K,\eta}^4/\Lambda_\chi^3$ corrections to the baryon masses. The other seven LECs correspond to interactions of the baryons with the axial current, of the form $\text{Tr}(\bar{B}\mathcal{A}\cdot\mathcal{A}B)$, and give rise to baryon mass corrections of the form $M_{\pi,K,\eta}^4 \ln(M_{\pi,K,\eta}^2)/\Lambda_\chi^3$. The lattice data used in this work, Ref. [27], are not sufficient to precisely determine all these LECs. Further, the number of LECs for which the mass relations are non-linearly dependent increases to four. In performing the full analysis, we use the VarPro method to reduce the number of LECs minimized numerically to 9. To perform the partial NNLO analysis, we add only the $\mathcal{O}(m_q^2)$ operators and are able to reduce the LECs which require numerical minimization to D and F , as in the NLO analysis.

In Fig. 19 we display the χ^2 vs D and F analyzed with the continuum $SU(3)$ extrapolation formula. In Fig. 20, we display the plot but with the mixed action extrapolation formula. In both cases, the five lightest ensembles are used, m007–m040. As can be seen, although the val-

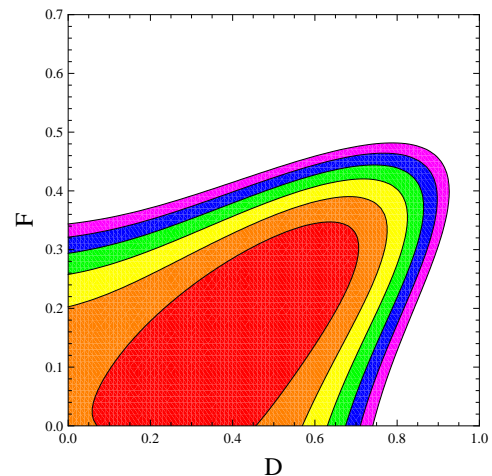


FIG. 19: $SU(3)$ heavy baryon analysis with NNLO counterterms added, as discussed in text.

ues of D and F are still consistent with zero, they are also now consistent with the phenomenological and lattice determined values, albeit with large uncertainties. This large allowed variation of D and F translate into about an order of magnitude increase in the uncertainties of the predicted baryon mass relations as compared to those in Table V. The full NNLO analysis yields results in qualitative agreement with the partial NNLO minimization.

This analysis makes it seem plausible that a combined NNLO analysis of the baryon masses and the axial couplings could provide much more stringent constraints on

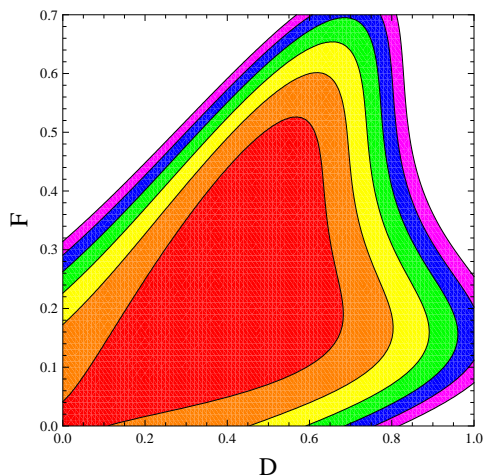


FIG. 20: Mixed action heavy baryon analysis with NNLO counterterms added, as discussed in text.

the values of D and F , as well as the other LECs. This would allow for the first rigorous exploration of octet and decuplet properties using $SU(3)$ heavy baryon chiral perturbation theory.

VI. CONCLUSIONS

In this work, we have explored $1/N_c$ baryon mass relations using lattice QCD. Some of these relations were derived assuming approximate $SU(3)$ flavor symmetry, M_1-M_8 , while other relations were derived assuming only $SU(2)$ flavor symmetry, M_A-M_D . In all cases, we have found that the baryon mass relations are of the size expected by both the $1/N_c$ power counting as well as the power counting in the $SU(3)$ breaking parameter, $\epsilon = (M_K^2 - M_\pi^2)/\Lambda_\chi^2$. In particular, for the mass relations M_A-M_D , it would be interesting to explore these relations with strange quark values even heavier than those used in this work. These relations must go to the equivalent heavy quark baryon relations as $m_s \rightarrow \infty$, and this exploration would probe the transition region between $m_s/\Lambda_{\text{QCD}} < 1 \rightarrow m_s/\Lambda_{\text{QCD}} > 1$. In the charmed and bottom baryon spectra, these $1/N_c$ relations have led to stringent predictions for various mass combinations. It would also be interesting to study M_1-M_8 , which were derived assuming an approximate $SU(3)$ flavor symmetry, as the strange quark mass is increased, to see when the perturbative $SU(3)$ expansion breaks down.

Due to the definite spin-flavor transformation properties of the baryon mass relations, the discretization cor-

rections to the mass relations also obey the $1/N_c$ and ϵ power counting, and are suppressed. In fact, only M_1 is subject to the leading $\mathcal{O}(a^2)$ mass corrections. The suppression of these discretization errors leads to more stringent constraints on the $SU(3)$ heavy baryon chiral extrapolation of the mass relations to the physical point, and a better method for chiral extrapolation. It allows one to rigorously test the predictions and convergence of $SU(3)$ HB χ PT.

In this work, we have also performed both $SU(3)$ and mixed-action chiral extrapolations of these mass relations using a variable projected χ^2 minimization. Consistent with other works, including Ref. [27] (from which our numerical data are produced), we find that a NLO analysis, which includes the leading non-analytic mass corrections, returns values of the axial couplings which are significantly smaller than expected from either phenomenology or lattice QCD. However, the predicted values of the mass relations, as well as the octet and decuplet masses themselves, are in good agreement with experiment. Further, we have shown that the partial inclusion of NNLO mass corrections returns values of the axial couplings, D and F which are consistent with expectations, albeit with large error bars.

Unfortunately, the data set we have used in this work is insufficient to precisely constrain all the LECs in the full NNLO analysis. However, we have demonstrated that a simultaneous extrapolation of both the hyperon axial couplings as well as the $1/N_c$ mass relations would allow for a rigorous exploration of the predictions and convergence of $SU(3)$ heavy baryon χ PT. It is possible, perhaps even likely, that the strange quark is too heavy for the $SU(3)$ theory to be convergent. This outcome, however, fails to explain the successes of flavor $SU(3)$ symmetry observed in nature in the baryon sector. Thus, a detailed study of this phenomena is warranted.

Acknowledgments

We would like to thank the members of the LHP Collaboration for providing their numerical baryon mass data of Ref. [27]. AWL would like to thank Kostas Orginos for helpful discussions. The work of EEJ and AVM was supported in part by the Department of Energy under Grant DE-FG03-97ER40546. The work of JWN was supported in part by the U. S Department of Energy under Grant DE-FG02-94ER40818. The work of AWL was supported in by the U.S. DOE OJI grant DE-FG02-07ER41527.

-
- [1] G. 't Hooft, Nucl. Phys. B **72**, 461 (1974).
 [2] E. Witten, Nucl. Phys. B **160**, 57 (1979).
 [3] S.R. Coleman, $1/N$, Presented at 1979 Int. School of Sub-

- nuclear Physics, Pointlike Structures Inside and Outside Hadrons, Erice, Italy, 1979.
 [4] R. F. Dashen and A. V. Manohar, Phys. Lett. B **315**,

- 425 (1993); B **315**, 438 (1993).
- [5] E. E. Jenkins, Phys. Lett. B **315**, 441 (1993); B **315**, 431 (1993); B **315**, 447 (1993).
- [6] R. F. Dashen, E. E. Jenkins and A. V. Manohar, Phys. Rev. D **49** (1994) 4713.
- [7] M. A. Luty and J. March-Russell, Nucl. Phys. B **426** (1994) 71
- [8] C. Carone, H. Georgi and S. Osofsky, Phys. Lett. B **322**, 227 (1994).
- [9] R. F. Dashen, E. E. Jenkins and A. V. Manohar, Phys. Rev. D **51** (1995) 3697.
- [10] D. Pirjol and T. M. Yan, Phys. Rev. D **57**, 1449 (1998).
- [11] C. L. Schat, J. L. Goity and N. N. Scoccola, Phys. Rev. Lett. **88**, 102002 (2002).
- [12] D. Pirjol and C. Schat, Phys. Rev. D **67**, 096009 (2003).
- [13] E. E. Jenkins, Ann. Rev. Nucl. Part. Sci. **48** (1998) 81.
- [14] A. V. Manohar, *Large N QCD*, Les Houches Summer School in Theoretical Physics, Session 68: Probing the Standard Model of Particle Interactions, Les Houches, France, 1997, arXiv:hep-ph/9802419.
- [15] E. E. Jenkins and R. F. Lebed, Phys. Rev. D **52** (1995) 282.
- [16] E. E. Jenkins, Phys. Rev. D **54** (1996) 4515, D **55** (1997) 10, D **77** (2008) 034012.
- [17] S. Durr *et al.*, Science **322**, 1224 (2008).
- [18] R. Flores-Mendieta *et al.*, Phys. Rev. D **62**, 034001 (2000).
- [19] M. J. Teper, Phys. Rev. D **59**, 014512 (1999).
- [20] M. J. Teper, *Large N*, arXiv:0812.0085 [hep-lat].
- [21] A. D. Kennedy, Nucl. Phys. Proc. Suppl. **140**, 190 (2005).
- [22] S. Aoki *et al.* [PACS-CS Collaboration], arXiv:0807.1661 [hep-lat].
- [23] E. E. Jenkins, A. V. Manohar and M. B. Wise, Phys. Rev. Lett. **75** (1995) 2272.
- [24] S. R. Beane, K. Orginos and M. J. Savage, Phys. Lett. B **654**, 20 (2007) [arXiv:hep-lat/0604013].
- [25] E. E. Jenkins and A. V. Manohar, Phys. Lett. B **255**, 558 (1991); **259**, 353 (1991).
- [26] A. Manohar and H. Georgi, Nucl. Phys. B **234** (1984) 189.
- [27] A. Walker-Loud *et al.*, Phys. Rev. D **79**, 054502 (2009).
- [28] D. B. Kaplan, Phys. Lett. B **288**, 342 (1992).
- [29] Y. Shamir, Nucl. Phys. B **406**, 90 (1993).
- [30] V. Furman and Y. Shamir, Nucl. Phys. B **439**, 54 (1995).
- [31] K. Orginos and D. Toussaint [MILC collaboration], Phys. Rev. D **59**, 014501 (1999).
- [32] K. Orginos, D. Toussaint and R. L. Sugar [MILC Collaboration], Phys. Rev. D **60**, 054503 (1999).
- [33] C. W. Bernard *et al.*, Phys. Rev. D **64**, 054506 (2001).
- [34] A. Bazavov *et al.*, arXiv:0903.3598 [hep-lat].
- [35] S. R. Beane, K. Orginos and M. J. Savage, Int. J. Mod. Phys. E **17**, 1157 (2008).
- [36] C. Aubin *et al.* [HPQCD Collaboration and MILC Collaboration and UKQCD Collaboration], Phys. Rev. D **70**, 031504 (2004).
- [37] C. Aubin *et al.*, Phys. Rev. D **70**, 094505 (2004).
- [38] C. Amsler *et al.* [Particle Data Group], Phys. Lett. B **667** (2008) 1.
- [39] E. E. Jenkins, Nucl. Phys. B **368**, 190 (1992).
- [40] R. F. Lebed and M. A. Luty, Phys. Lett. B **329**, 479 (1994).
- [41] B. Borasoy and U. G. Meissner, Annals Phys. **254**, 192 (1997).
- [42] A. Walker-Loud, Nucl. Phys. A **747**, 476 (2005).
- [43] R. F. Lebed, Nucl. Phys. B **430**, 295 (1994).
- [44] B. C. Tiburzi and A. Walker-Loud, Nucl. Phys. A **748**, 513 (2005).
- [45] J. W. Chen and M. J. Savage, Phys. Rev. D **65**, 094001 (2002).
- [46] B. C. Tiburzi, Phys. Rev. D **72**, 094501 (2005).
- [47] J. W. Chen, D. O'Connell and A. Walker-Loud, JHEP **0904**, 090 (2009).
- [48] K. Orginos and A. Walker-Loud, Phys. Rev. D **77**, 094505 (2008).
- [49] G. Golub and V. Pereyra, Inverse Problems, **19**, R1-R26 (2006).
- [50] R. Flores-Mendieta, E. E. Jenkins and A. V. Manohar, Phys. Rev. D **58**, 094028 (1998); J. Dai, *et al.*, Phys. Rev. D **53**, 273 (1996).
- [51] H. W. Lin and K. Orginos, Phys. Rev. D **79**, 034507 (2009).
- [52] A. Walker-Loud, arXiv:0810.0663 [hep-lat].